

Chapter 2

Histologic Anatomy

Blythe Gorman

Esophageal Pathology

Cytologic sampling and tissue biopsy of the esophagus should be considered in the context of the patient's history and endoscopic findings. The location of the lesion in the esophagus, the endoscopic appearance of the lesion, and any other clinical or endoscopic findings are all valuable data points to the pathologist.

Some lesions are better sampled by cytologic brushing rather than with biopsy forceps. Brush cytology, for example, is far more sensitive for the detection of *Candida* than tissue biopsy. Tissue biopsy is usually superior to cytologic brushing in the case of suspected carcinoma, as the depth of invasion and presence or absence of a desmoplastic stromal response cannot be assessed by cytologic sampling alone. Cytologic sampling of esophageal and gastroesophageal lesions is complementary to tissue biopsy.

This chapter covers the basic gross features as well as the cyto- and histopathology of commonly encountered esophageal lesions.

B. Gorman, MD
Department of Pathology and Genomic Medicine, Weill Cornell Medical College,
Houston Methodist Hospital,
6565 Fannin Street, M227, Houston, TX 77030, USA
e-mail: BKGorman@houstonmethodist.org

© Springer Science+Business Media New York 2015
S.H. Blackmon et al. (eds.), *Atlas of Esophageal Disease and Intervention:
A Multidisciplinary Approach*, DOI 10.1007/978-1-4939-3088-3_2

Normal Esophagus

The innermost layer of the normal esophagus is composed of epithelium bounded by a basement membrane (Figs. 2.1, 2.2, and 2.3). The epithelium rests on top of the lamina propria, which contains lymphatic channels. The muscularis mucosa is the deepest layer of the mucosa, beneath which is the submucosa. The submucosa also contains submucosal glands, ducts and lymphatic channels. The muscularis propria consists of an inner circular layer and an outer longitudinal layer of smooth muscle. The adventitia is the outermost lining of the esophagus, which lacks a serosal surface [1].



Fig. 2.1 Normal distal esophagus, gastroesophageal (GE) junction, and stomach after formalin fixation. The squamous mucosa is pinkish white, the GE junction is well demarcated, and the stomach shows normal darker pink columnar mucosa with rugae

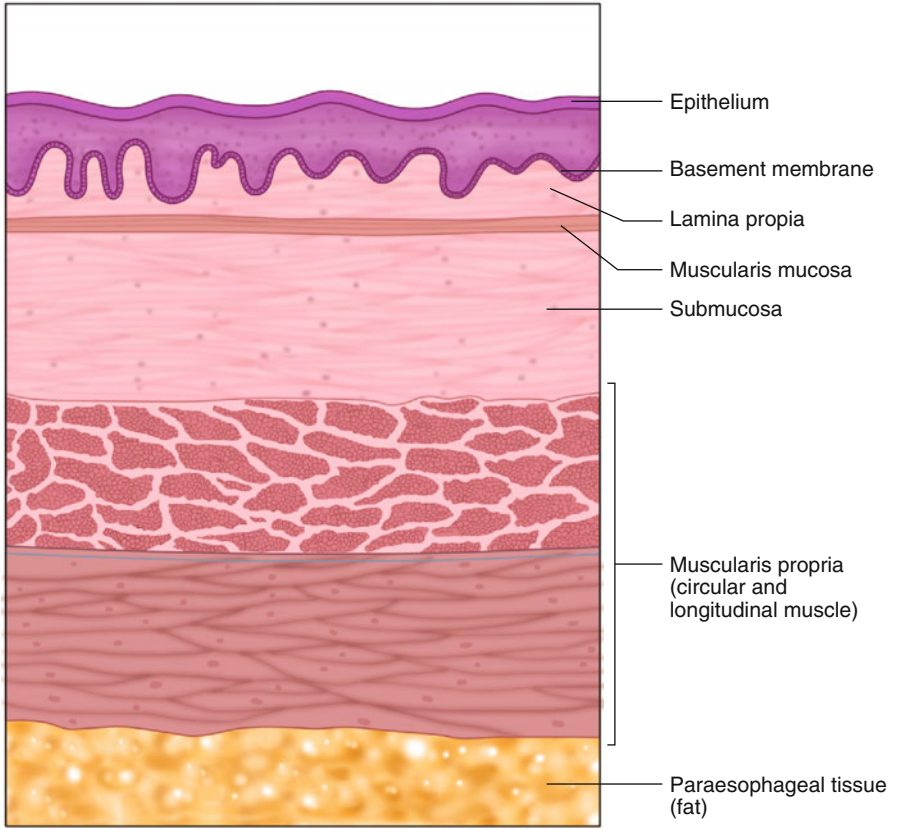


Fig. 2.2 Schematic view of a normal full-thickness section of esophagus

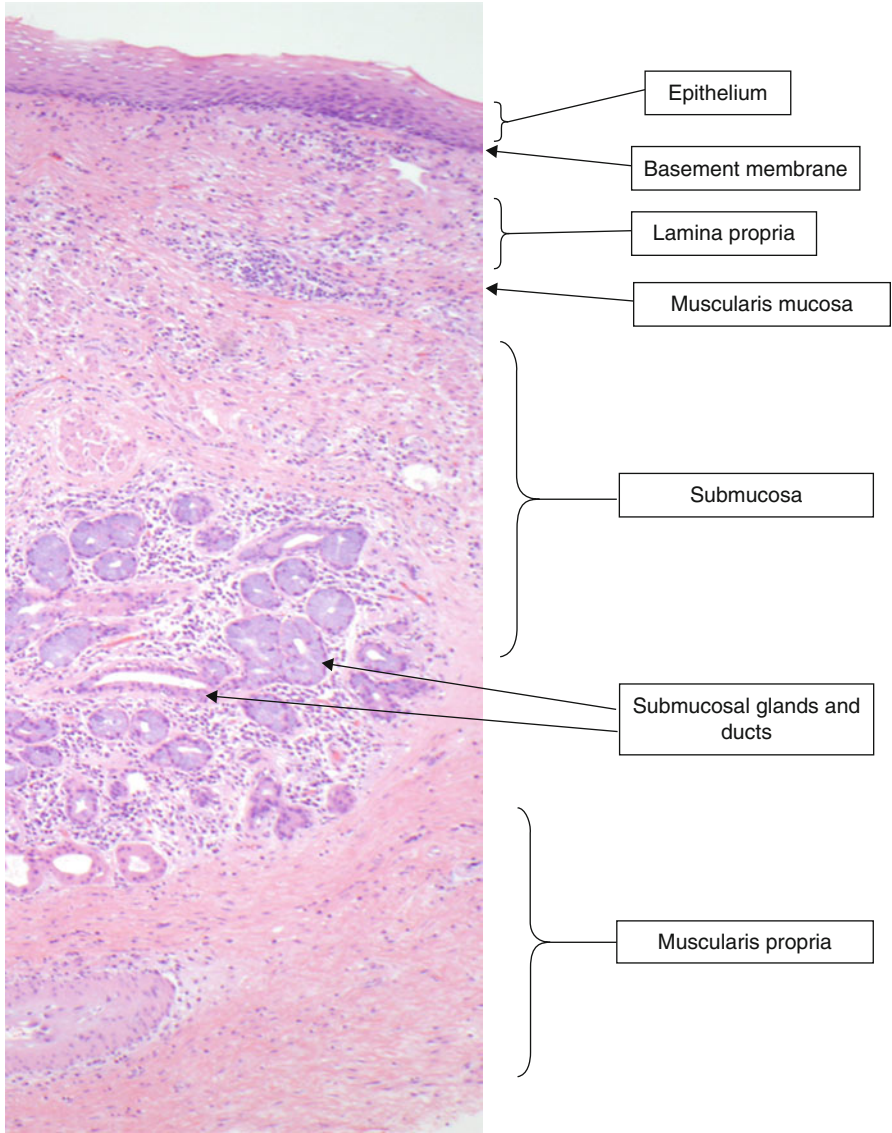


Fig. 2.3 Normal histology of a full-thickness section of esophagus (hematoxylin-eosin [H & E], $\times 20$)

Esophagitis

Changes of reflux esophagitis include thickening/proliferation of the epithelial basal cell layer with dilated intracellular spaces, elongated lamina propria papillae, and intraepithelial eosinophils (Fig. 2.4a).

Increased lymphocytes may be seen in the epithelium and lamina propria (Fig. 2.4b) [2]. Note the dilated intercellular spaces (spongiosis), reflective of intercellular edema. The nuclei have reactive changes including enlargement and prominent nucleoli with retention of smooth nuclear and nucleolar contours.

Multilayered epithelium (Fig. 2.4c) is characterized by the presence of columnar glandular cells overlying squamous cells. This change is associated with reflux esophagitis, but also may be seen in biopsy specimens taken from patients who go on to develop Barrett's esophagus, as reflux is often seen in these patients as well [3].

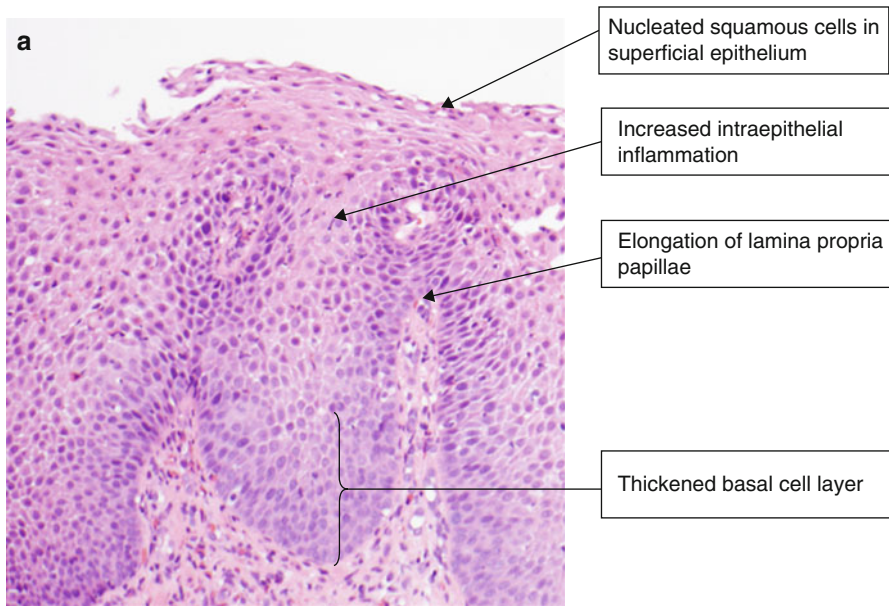


Fig. 2.4 Histology of esophagitis. (a) Reflux esophagitis (H & E, $\times 100$). (b) Reflux esophagitis, basal layer of epithelium (H & E, $\times 400$). (c) Gastroesophageal junction with multilayered epithelium (H & E, $\times 400$)

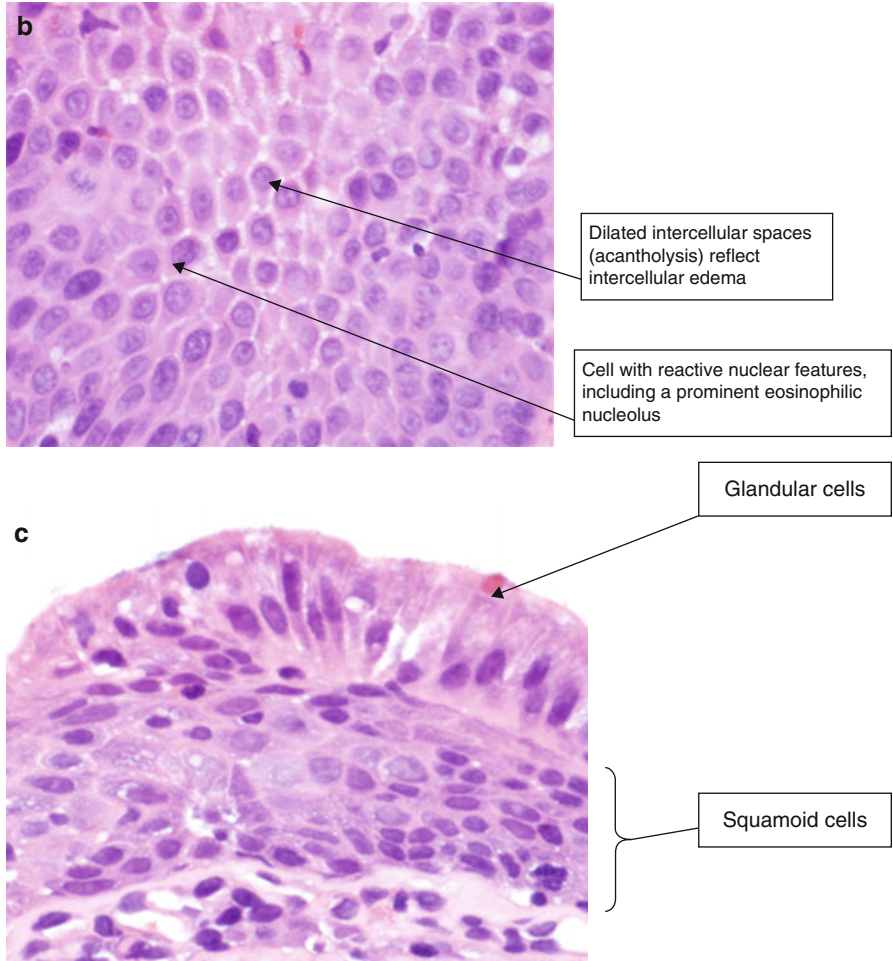


Fig. 2.4 (continued)

Barrett's Esophagus

The squamocolumnar junction is composed of squamous epithelium and glandular epithelium (Figs. 2.5 and 2.6a). In the United States, Barrett's metaplasia is defined by the presence of columnar epithelium with goblet cells. The metaplastic epithelium must be located in the tubular esophagus. The goblet cells are distended by blue-hued acid mucin. Note that the epithelium is mature at the surface, as the cells have abundant cytoplasm and small nuclei that are oriented toward the basement membrane. No dysplasia is seen Fig. 2.6a.

Another feature of Barrett's esophagus is duplication of the muscularis mucosa (Fig. 2.6b). The original muscularis mucosa is located deeper than the new layer that is associated with Barrett's esophagus. The new layer is closer to the lumen of the esophagus and is composed of thinner, frayed smooth muscle fibers. There may be edematous lamina propria between the two layers.

A diagnosis of Barrett's esophagus indefinite for dysplasia may be rendered under several circumstances. In Fig. 2.7a, for example, glands lined by atypical, metaplastic epithelium are seen beneath squamous epithelium; they are "buried." This neopithelialization may occur after radiofrequency ablation treatment of Barrett's esophagus. The glandular cells have nuclear hyperchromasia and enlargement, some stratification, and increased mitotic activity. The degree of surface maturation of the glandular epithelium cannot be assessed in this sample because of the overgrowth of squamous epithelium. As a definitive diagnosis of dysplasia cannot be rendered, the diagnosis of "indefinite for dysplasia" is felt most appropriate. However, the mere presence of buried metaplastic epithelium is insufficient to warrant a diagnosis of indefinite for dysplasia.

Other situations that may warrant a diagnosis of indefinite for dysplasia include: (1) the presence of marked reactive atypia in the setting of ulceration or inflammation; (2) atypia limited to the bases of the glands (not extending to involve the surface epithelium); (3) tangential sectioning, absence of surface epithelium, or other artifactual changes; and (4) cytologic and architectural changes that are worrisome for, but not diagnostic of, dysplasia (Fig. 2.7b) [3].

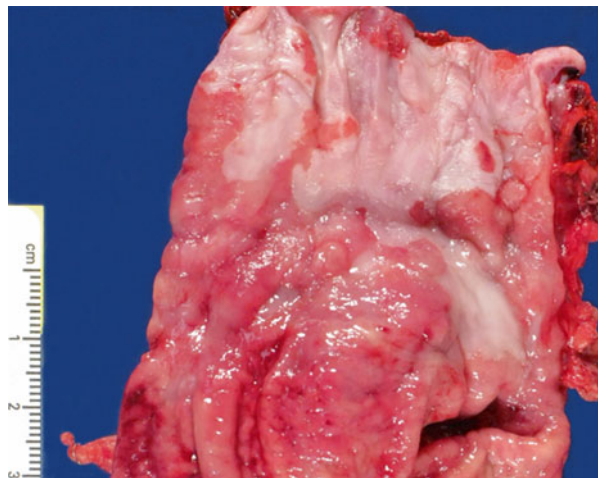


Fig. 2.5 Gross photo of gastroesophageal junction with Barrett's esophagus (fresh specimen)

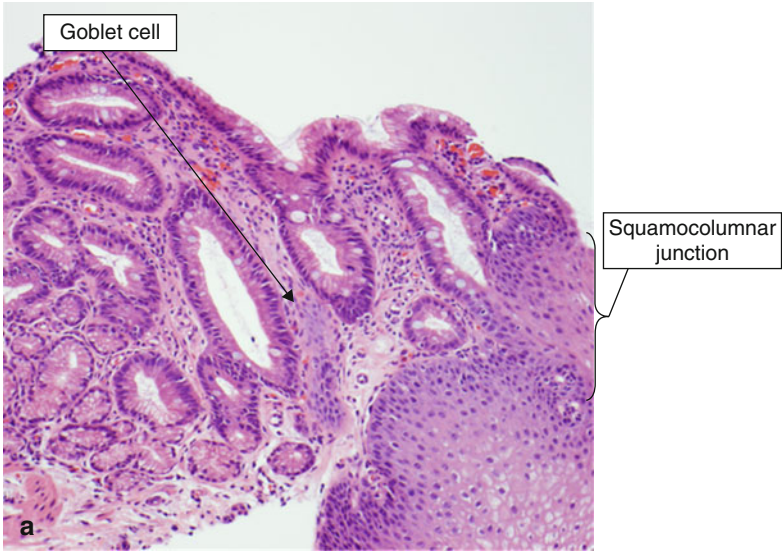


Fig. 2.6 Barrett's esophagus, histology. (a) Barrett's esophagus (H & E, $\times 100$). (b) Barrett's esophagus (H & E, $\times 40$)

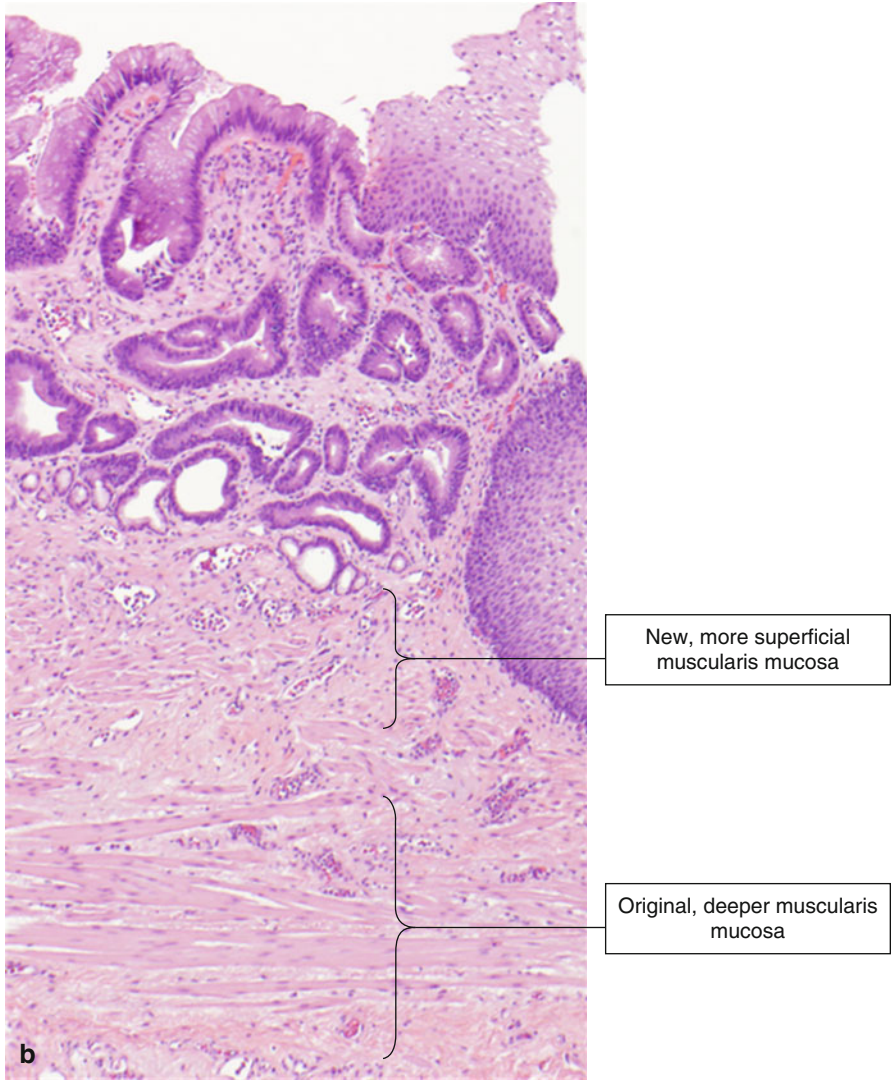
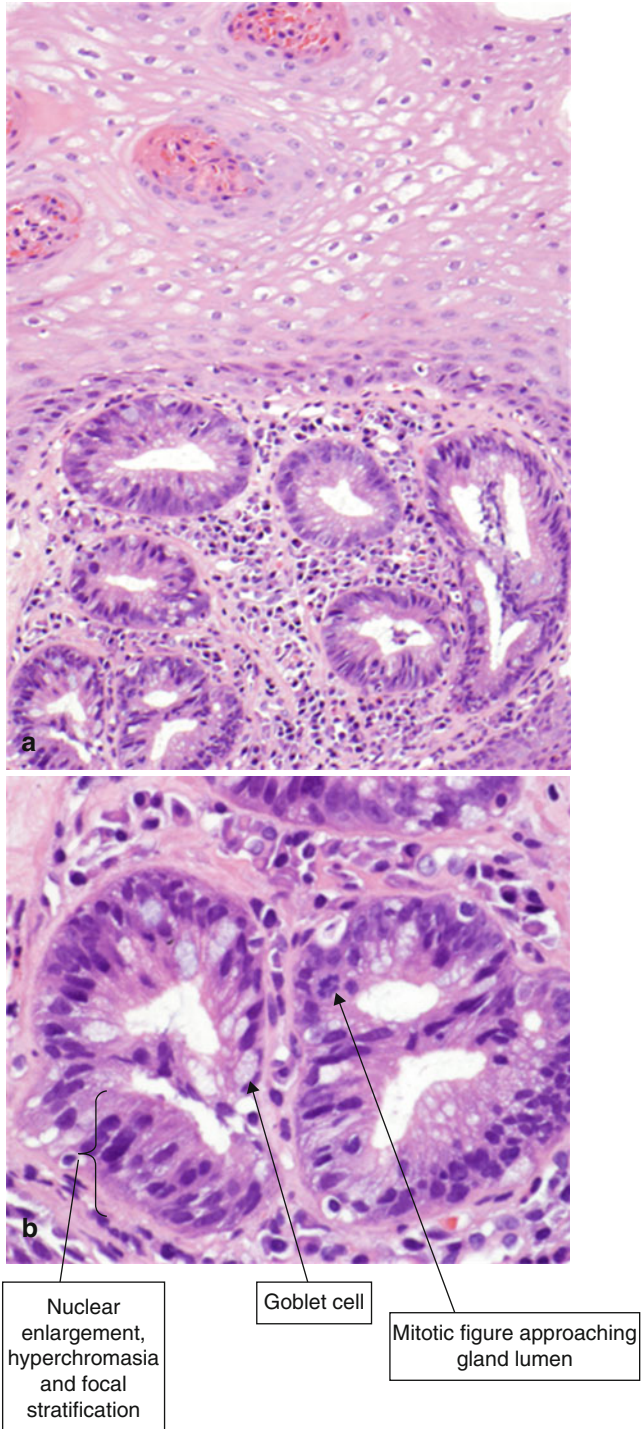


Fig. 2.6 (continued)

Fig. 2.7 (a) Barrett's esophagus, indefinite for dysplasia (H & E, $\times 100$). (b) Barrett's esophagus, indefinite for dysplasia (H & E, $\times 400$). The cells show cytologic features of dysplasia that include nuclear enlargement, hyperchromasia, and some nuclear stratification. Diagnostic features of high-grade dysplasia are not seen



Barrett's Esophagus, Low-Grade Dysplasia

Low-grade dysplasia is characterized by nuclear crowding, stratification, atypia, and increased mitotic figures (Fig. 2.8). The atypical nuclei extend beyond the crypt epithelium to involve the superficial epithelium. Focal goblet-cell depletion may also occur. The contours of the dysplastic glands are more irregular than those without dysplasia. In contrast to high-grade dysplasia, low-grade dysplasia retains some nuclear polarity (most nuclei are oriented toward the basal aspect of the cell, away from the luminal surface) and the nuclei remain elongated or cigar-shaped.

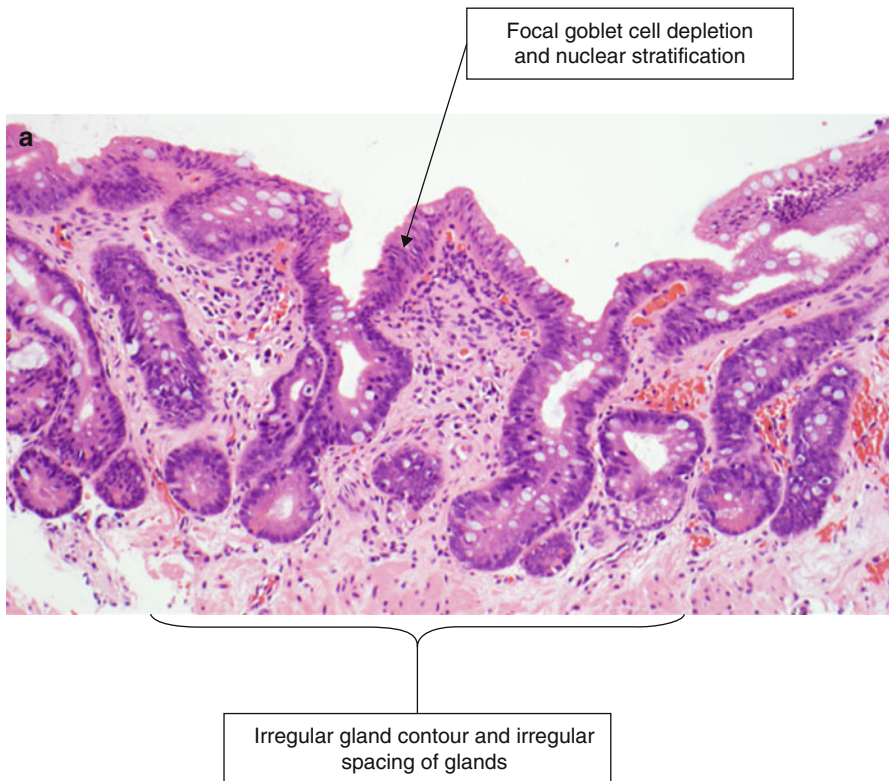


Fig. 2.8 (a) Barrett's esophagus, low-grade dysplasia (H & E, $\times 100$). (b) Barrett's esophagus, low grade dysplasia (H & E, $\times 200$). Review of the histological specimen by two histopathologists is recommended to diagnose and characterize dysplasia in Barrett's esophagus

Note the absence of goblet cells in the portion of the epithelium. The nuclei are stratified and approach the luminal border but are still elongated. In low grade dysplasia, the changes extend to the surface epithelium.

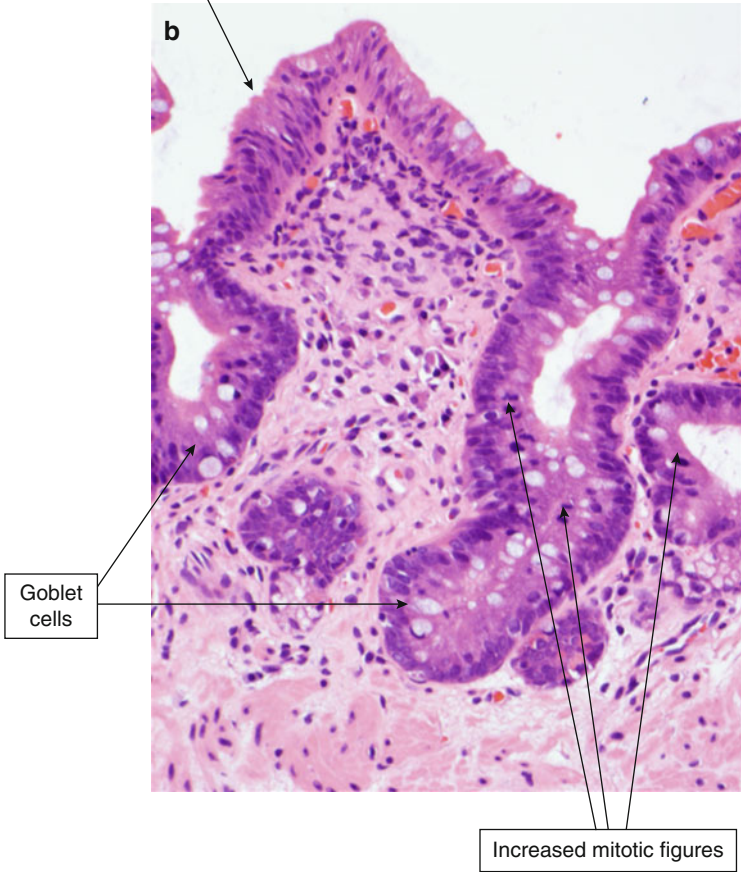


Fig. 2.8 (continued)

Barrett's Esophagus, High-Grade Dysplasia

High-grade dysplasia shows more marked nuclear atypia, which extends to the superficial epithelium (Fig. 2.9). The nuclei are hyperchromatic, enlarged, and rounded, often with irregular nuclear contours. There is loss of nuclear polarity, often with full-thickness nuclear stratification. Increased mitotic figures (including atypical forms) are seen, and goblet cells are notably decreased. Some features, when present in biopsy specimens showing Barrett's esophagus with high-grade dysplasia, are predictive of invasive carcinoma upon surgical resection. These features include gland cribriforming, dilated glands with necrotic material, ulceration of high-grade dysplasia, invasion of dysplastic glands into the overlying squamous epithelium and the presence of many neutrophils within the epithelium with high grade dysplasia [4].

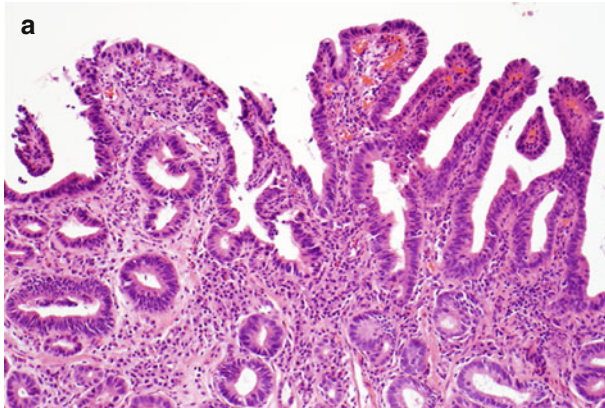


Fig. 2.9 (a) Barrett's esophagus, high-grade dysplasia (H & E, $\times 100$). (b) Barrett's esophagus, high-grade dysplasia (H & E, $\times 200$). (c) Barrett's esophagus, high-grade dysplasia (H & E, $\times 400$)

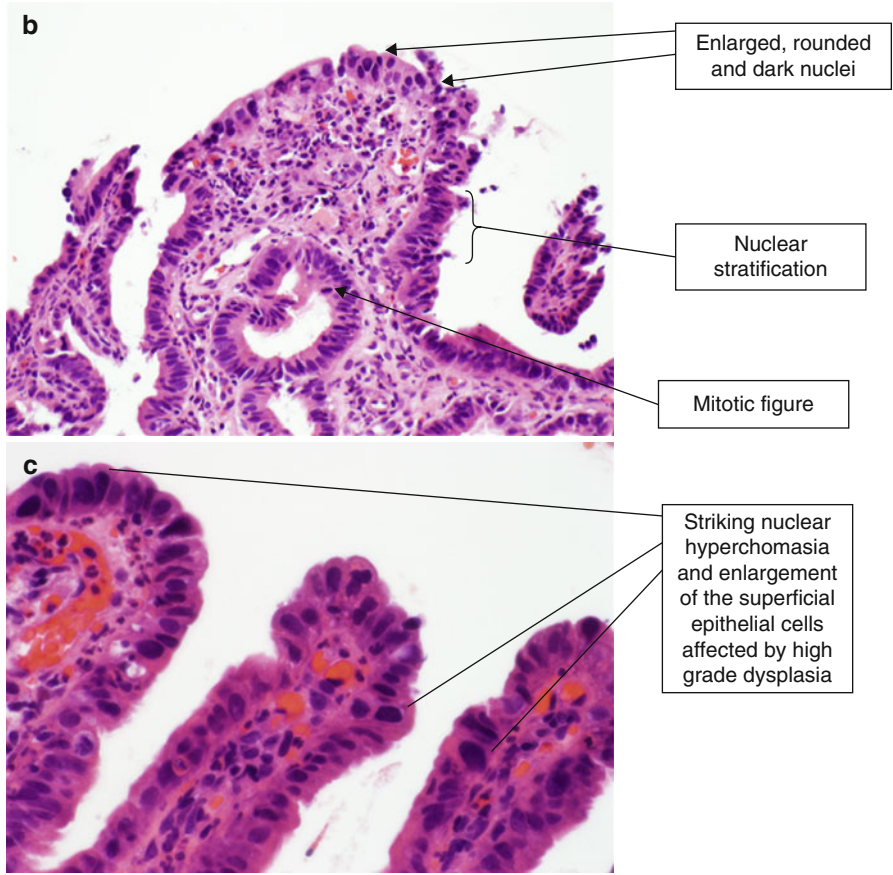


Fig. 2.9 (continued)

Adenocarcinoma

The presence of dysplastic glands beyond the epithelial basement membrane and within the lamina propria or duplicated muscularis mucosa defines intramucosal adenocarcinoma (Fig. 2.10). Invasion through the true muscularis mucosa and into the submucosa is not identified. The nuclear morphology is similar to that seen in high-grade dysplasia. The gland architecture is complex and crowded, with back-to-back glands lacking intervening stroma. Angular gland contours, intraluminal necrosis, and dilatation of gland lumina may also be seen. In addition, single malignant cells may be present within the lamina propria. As lymphatics are present in the lamina propria of the esophagus, there is a small risk of metastasis [5]. The histological diagnosis of intramucosal adenocarcinoma corresponds to T1a disease, with invasion into the lamina propria or muscularis mucosa. This finding is important, as the 15–20 % rate of lymph node metastases with submucosal tumors (T1b disease) is higher than the rate for T1a disease (5–7 %).

Adenocarcinoma of gastroesophageal junction is a bulky, nodular, and exophytic tumor. The surrounding gastric mucosa may be hemorrhagic (Fig. 2.11).

With esophageal adenocarcinoma, malignant glands invade deep into the muscularis propria (Fig. 2.12). Cribriform architecture and areas of necrosis are present. The overlying epithelium is dysplastic. Invasion into the muscularis propria defines this tumor as pT2 (seventh edition AJCC Cancer Staging Manual) [6].

Due to the large amount of extracellular mucin, mucinous adenocarcinoma is relatively less cellular than the other types (Fig. 2.13). Clusters of tumor cells are afloat in a sea of mucin. The overlying squamous epithelium is essentially normal. By definition, a diagnosis of mucinous carcinoma is rendered when more than 50 % of the lesion consists of mucin [7].

Fig. 2.10 (a) Intramucosal adenocarcinoma (H & E, $\times 100$).
(b) Intramucosal adenocarcinoma (H & E, $\times 200$)

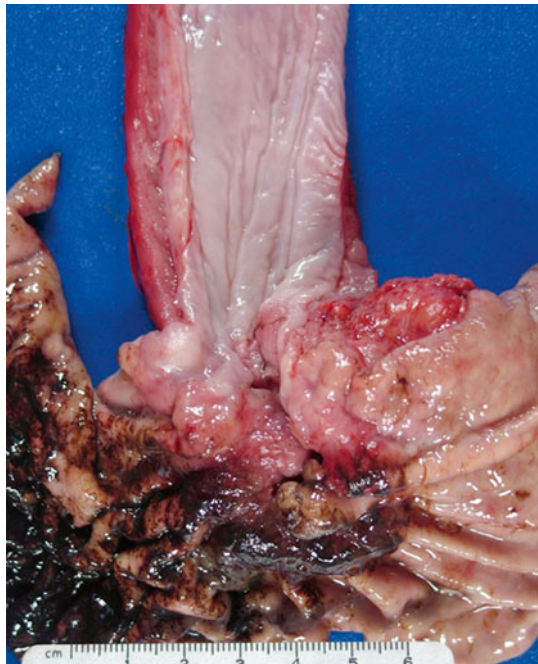
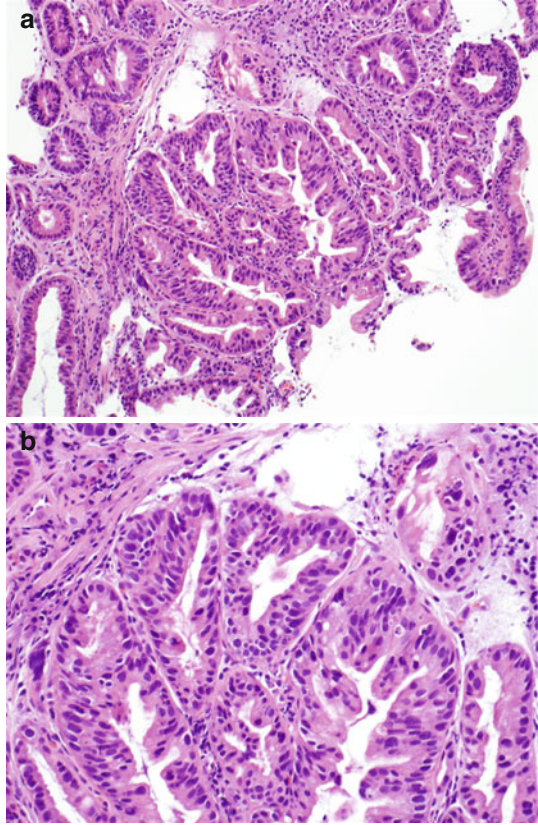


Fig. 2.11 Untreated adenocarcinoma at the gastroesophageal junction (fresh specimen)

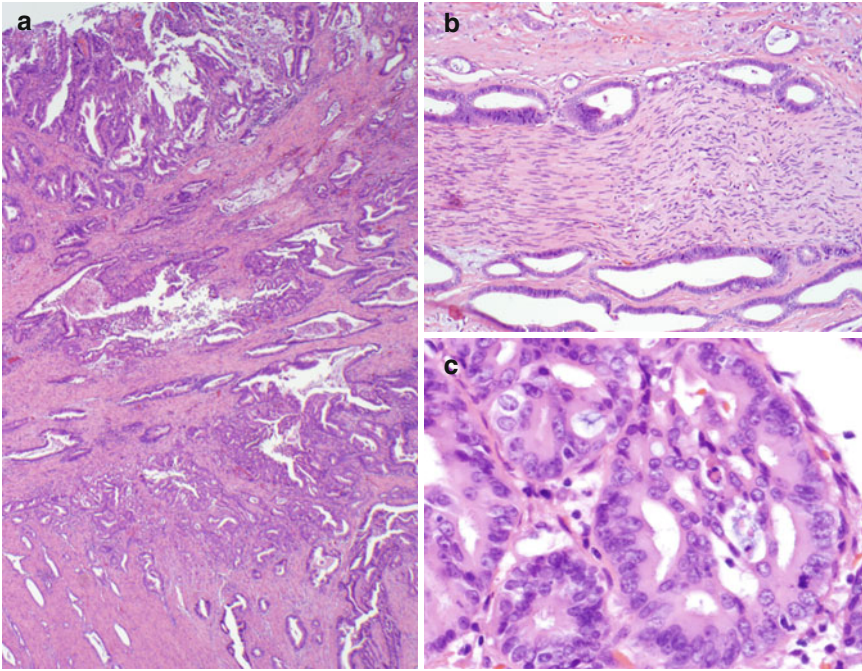


Fig. 2.12 Esophageal adenocarcinoma. (a) Adenocarcinoma (H & E, $\times 20$). (b) Adenocarcinoma showing perineural invasion (H & E, $\times 100$). (c) Adenocarcinoma with complex, cribriform architecture (H & E, $\times 400$). Note the irregular size and shape of gland lumina with intraluminal necrosis. The tumor cell nuclei are large, with prominent nucleoli

Fig. 2.13 Mucinous adenocarcinoma (a recurrence). (a) H & E, $\times 40$. Squamous epithelium overlies tumor cells in a background of mucin. (b) H & E, $\times 100$. Irregular nests of tumor cells infiltrate the stroma. (c) H & E, $\times 200$. (d) H & E, $\times 400$. Note the signet ring appearance of several tumor cells. This is due to intracytoplasmic mucin. Although some of the tumor cell nuclei are small, they are hyperchromatic, angular, and displaced by the mucin vacuoles

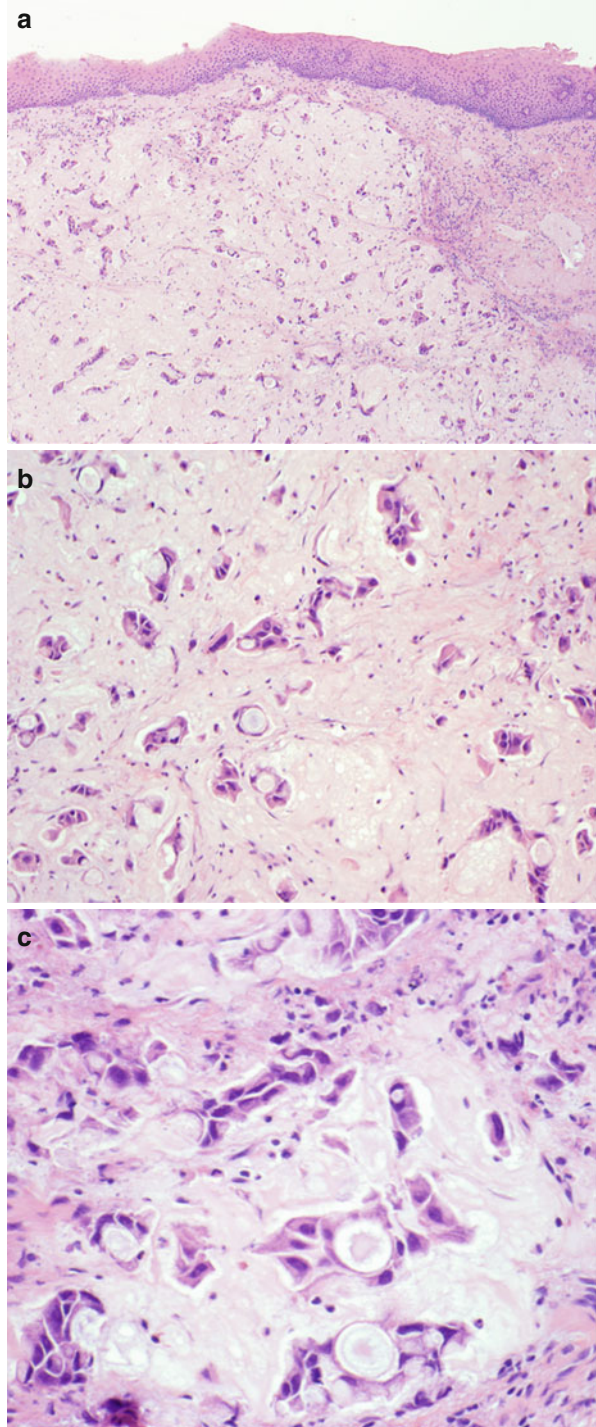
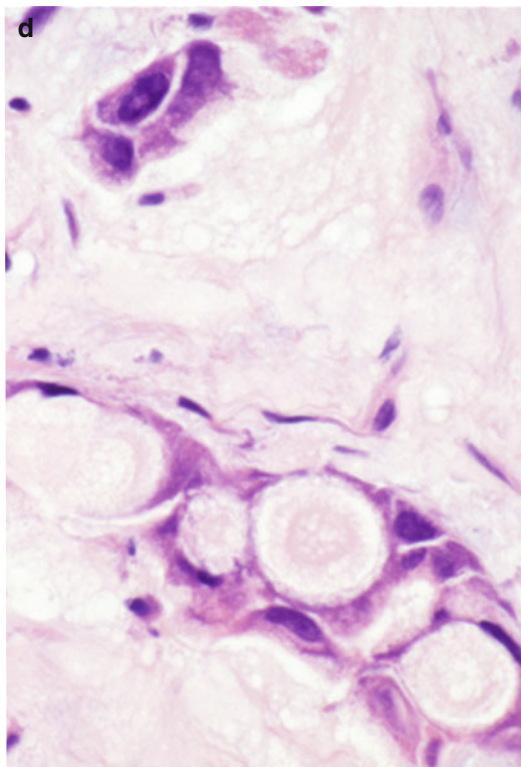


Fig. 2.13 (continued)



Esophageal Squamous Cell Carcinoma

The squamous cell carcinoma shown in Figs. 2.14 and 2.15 is ulcerative and infiltrates the wall of the esophagus. Note the thickening of the wall. The surface of the tumor is irregular and somewhat nodular but is well demarcated from the normal esophageal mucosa.

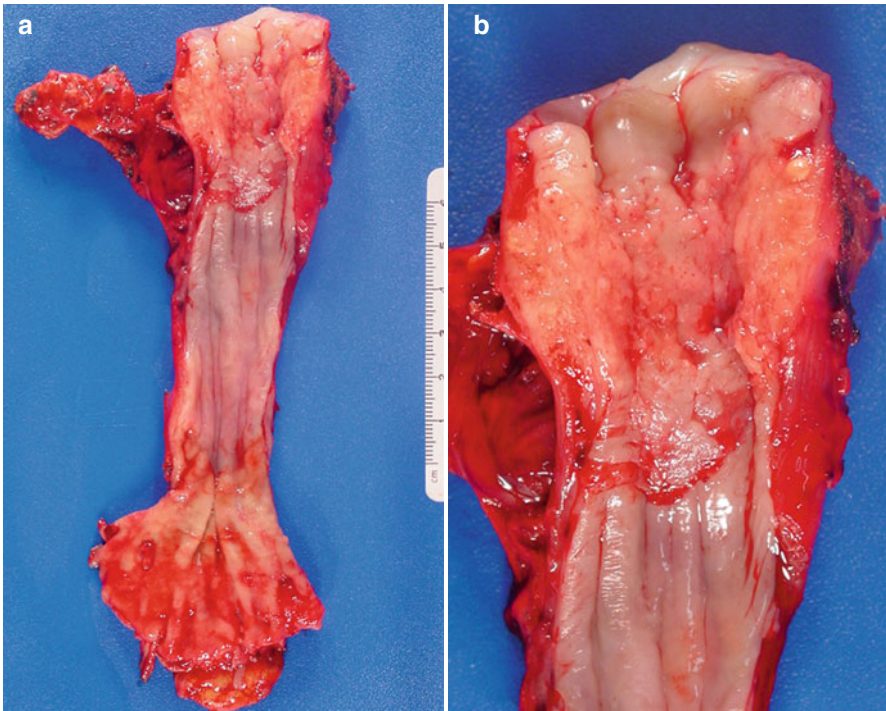
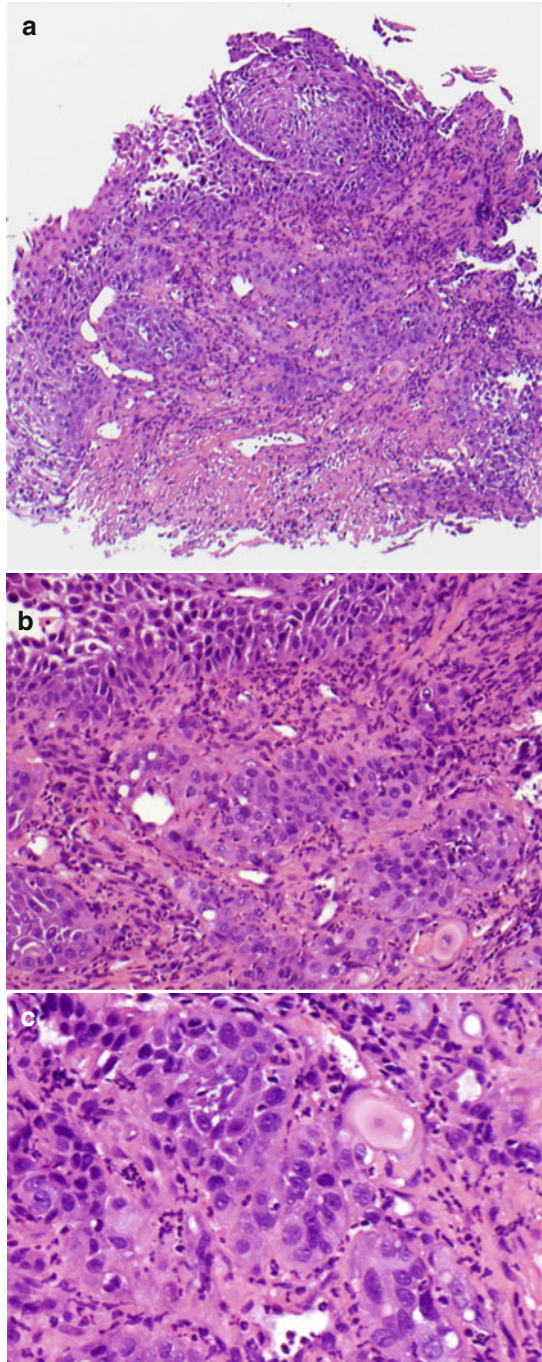


Fig. 2.14 (a, b) Esophageal squamous cell carcinoma, gross photos

Fig. 2.15 (a) Squamous cell carcinoma (H & E, $\times 40$). This moderately differentiated squamous cell carcinoma involves the full thickness of the biopsy specimen. Tumor necrosis is prominent. (b) Squamous cell carcinoma (H & E, $\times 200$). The tumor cells have enlarged hyperchromatic nuclei and infiltrate the stroma in irregular nests. (c) Squamous cell carcinoma (H & E, $\times 400$). The presence of intercellular bridges (delicate filaments seen between the tumor cells) indicates squamous differentiation, as does keratin production



Candida

The esophageal brushing specimen in Figs. 2.16 and 2.17 shows numerous *Candida* yeast and pseudohyphae. The pseudohyphae are said to skewer the squamous cells, giving a characteristic “shish kebab” appearance. The squamous cells show reactive changes that include nuclear enlargement and mild hyperchromasia. Cytologic specimens are often of higher yield than biopsies for detecting *Candida*, as the brush samples a larger surface area. Special stains are frequently employed to aid in the detection of organisms in both histologic and cytologic samples. Two of the more commonly used special stains for fungus are Gomori methenamine silver (GMS) and periodic acid–Schiff with diastase (PAS-D).

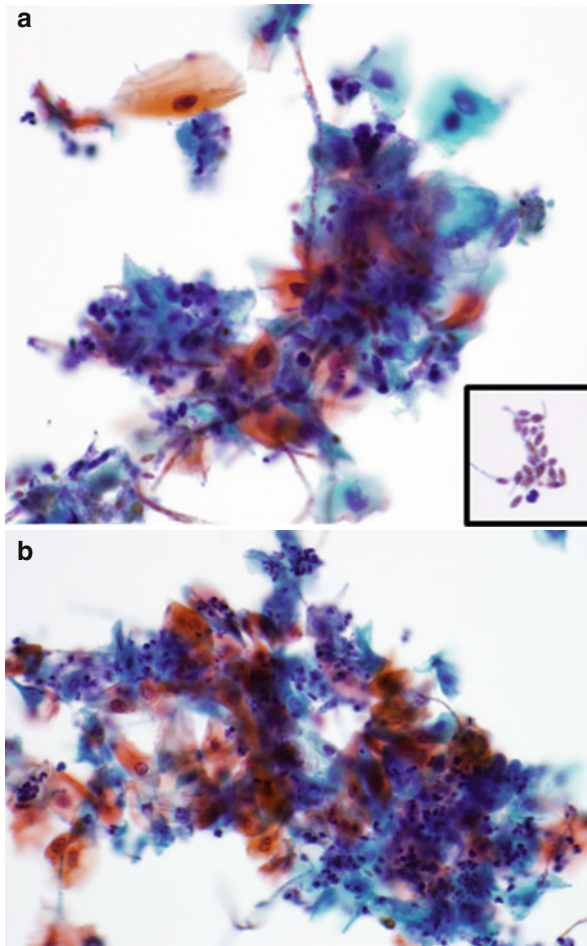


Fig. 2.16 *Candida* in an esophageal brushing specimen. (a) *Candida* species (ThinPrep, Papanicolaou stain, $\times 200$; inset $\times 400$). The inset panel shows a high-power view of the fungal yeast. (b) *Candida* species (100 \times , ThinPrep, Papanicolaou stain, $\times 100$)

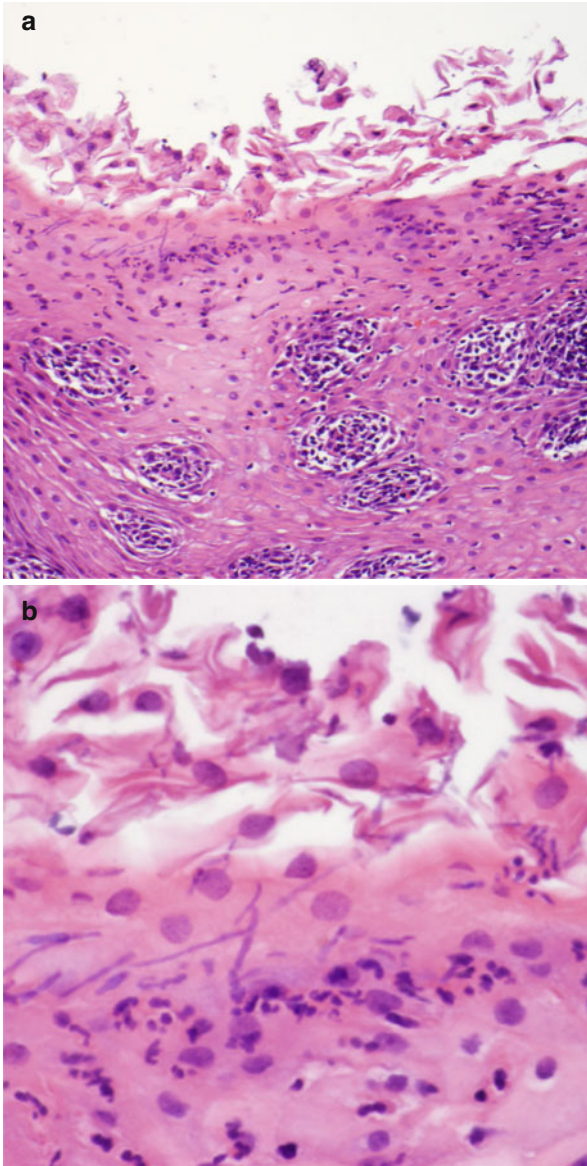


Fig. 2.17 (a) *Candida* esophagitis (H & E, ×100). This biopsy specimen shows squamous epithelium with increased intraepithelial acute and chronic inflammation. The presence of neutrophils in the epithelium is a clue to search for fungi. When numerous, the fungi are easily visible on H & E–stained sections. (b) *Candida* esophagitis (H & E, ×400)

Eosinophilic Esophagitis

In eosinophilic esophagitis, a myriad of eosinophils infiltrates the epithelium and the lamina propria (Fig. 2.18). Intraepithelial clusters of eosinophils (eosinophilic abscesses) and degranulation are characteristic. Features of reflux esophagitis are also seen (basal cell hyperplasia, dilated intercellular spaces, and elongation of the lamina propria papillae) [8]. Scattered eosinophils may be present in reflux esophagitis, but the amount seen in eosinophilic esophagitis is far greater. Some authors use a cutoff of at least 20 eosinophils per high-power field, but the exact number of eosinophils required for the diagnosis is debated and requires additional study [9].

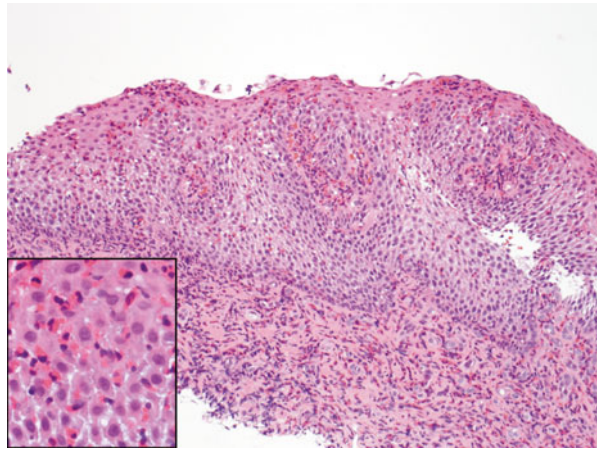


Fig. 2.18 Eosinophilic esophagitis (H & E, $\times 100$; inset $\times 400$)

Stricture

In stricture of the esophagus, the esophageal wall is thickened and fibrotic. Visualizing the mucosal surface may require using forceps to hold the specimen open (Fig. 2.19), unlike the specimens pictured in the other gross photographs.

Histology shows marked thickening and fibrosis of the lamina propria, submucosa, and muscularis propria (Fig. 2.20). (Compare the normal histology in Fig. 2.3, shown at the same magnification.)

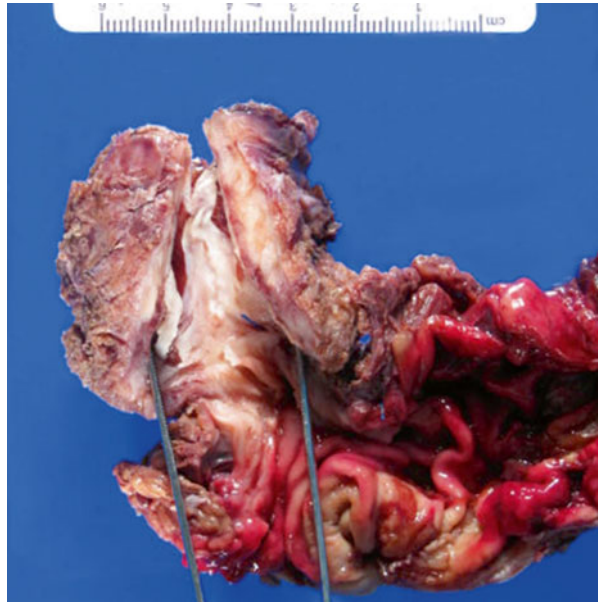
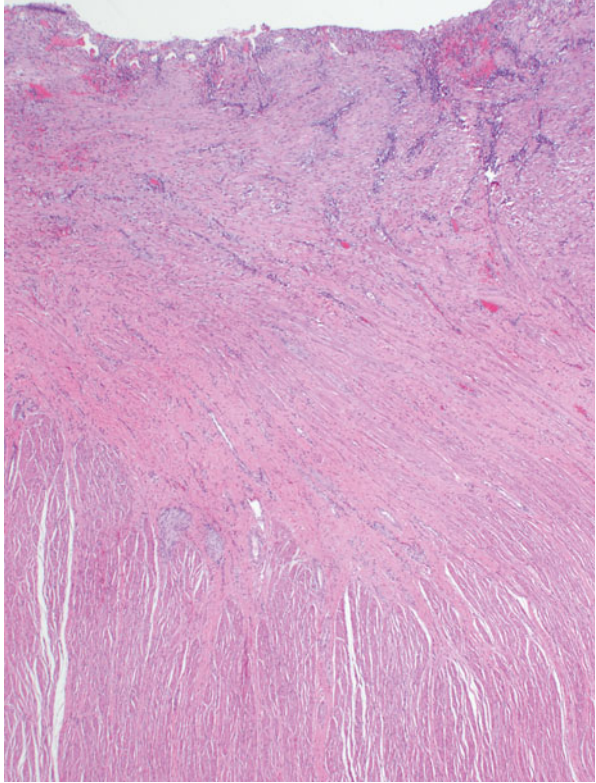


Fig. 2.19 Stricture of the esophagus, fresh specimen

Fig. 2.20 Histology of stricture (H & E, $\times 20$)



Inlet Patch

The inlet patch is characterized by ectopic gastric mucosa that is surrounded by normal squamous mucosa (Fig. 2.21). Inlet patches are most frequently seen in biopsy specimens taken from the upper third of the esophagus.

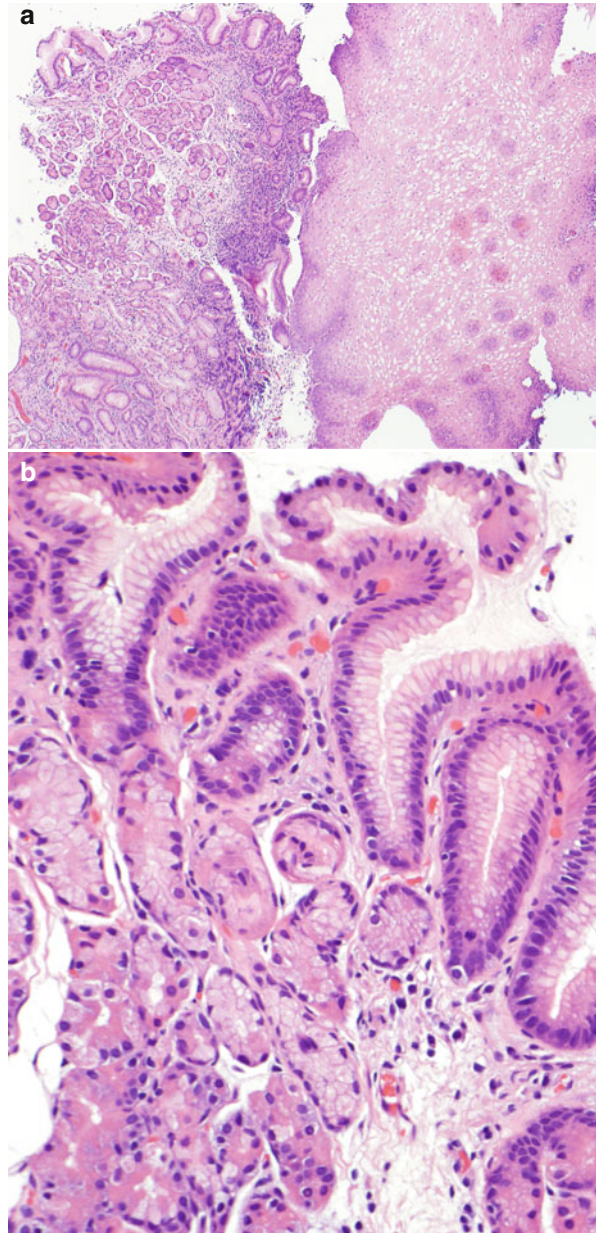


Fig. 2.21 (a) Inlet patch (H & E, $\times 40$). The mucosa on the left side of this photomicrograph shows essentially normal gastric mucosa with foveolar and glandular epithelium. The mucosa on the right shows normal esophageal squamous epithelium. (b) Inlet patch (H & E, $\times 200$). On higher power, the gastric mucosa of the inlet patch is identical to that seen in the stomach, with foveolar epithelium overlying gastric glands composed of mucus neck cells, parietal cells, and chief cells. Oxyntic-type gastric mucosa is most common, although antral and mixed type are also seen [10]

Achalasia

Achalasia, the failure of smooth muscle fibers (usually in the esophagus and lower esophageal sphincter) to relax, can cause dilatation of the distal esophagus. The examples of achalasia in Figs. 2.22 and 2.23 show dilatation of the distal esophagus with an area of ulceration at the gastroesophageal junction.

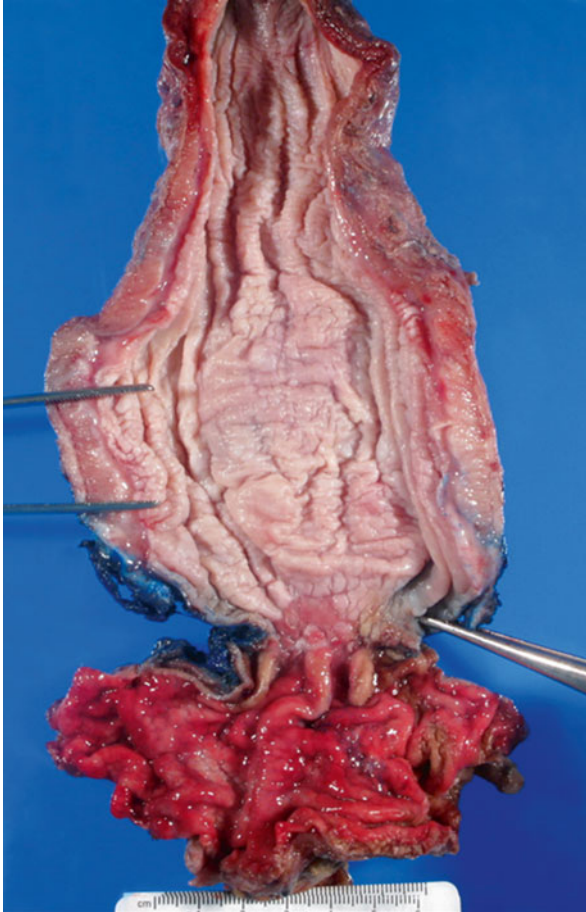


Fig. 2.22 Esophagogastrectomy specimen with achalasia, unfixed

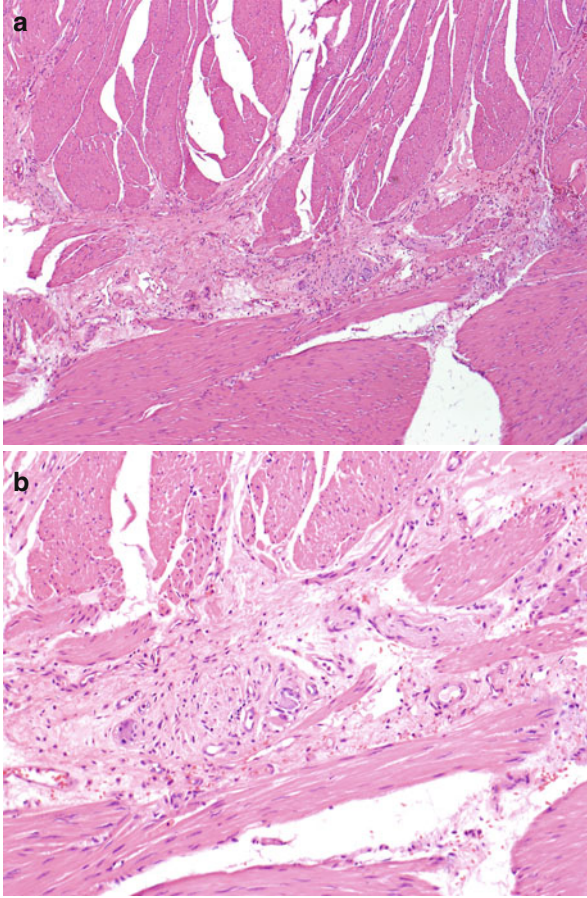


Fig. 2.23 (a) Achalasia (H & E, $\times 40$). Features of achalasia include fibrosis of the myenteric plexus and decreased numbers of ganglion cells. Smooth muscle hypertrophy and lymphoplasmacytic infiltration of the myenteric plexus may also be seen. (b) Achalasia (H & E, $\times 100$). A minimal lymphoplasmacytic infiltrate surrounds a small nerve in the myenteric plexus, located between the inner circular and outer longitudinal layers of the muscularis propria. The degree of inflammation depends in part upon the age of the lesion

Glycogen Accumulation

Glycogen accumulation creates cytoplasmic clearing in squamous cells (Fig. 2.24). This finding may mimic the perinuclear halo seen with the human papillomavirus cytopathic effect. The absence of characteristic nuclear changes supports a diagnosis of glycogen accumulation.

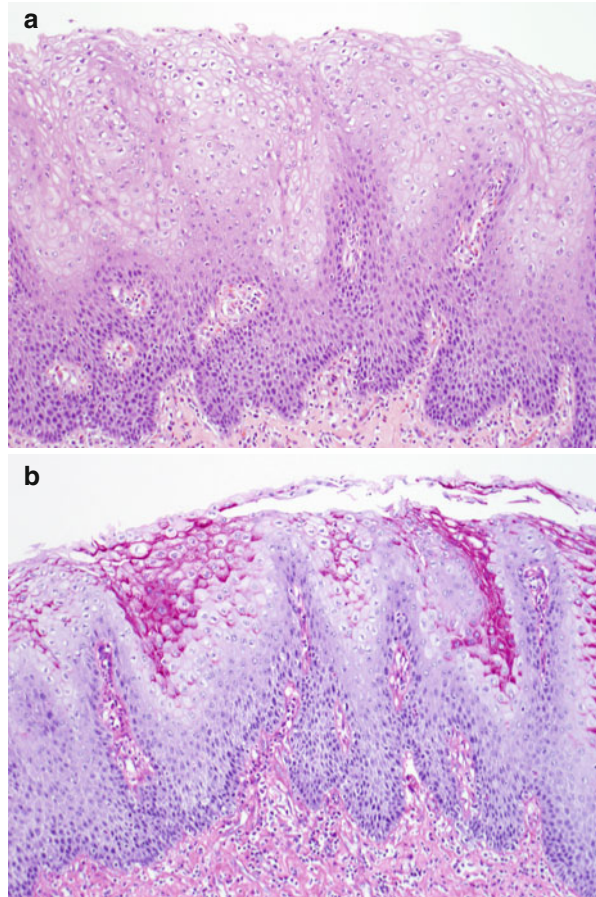


Fig. 2.24 (a) Glycogen accumulation (H & E, $\times 100$). (b) Glycogen accumulation (PAS without diastase, $\times 100$). The PAS stain highlights the cytoplasmic glycogen

Herpes Esophagitis

Herpesvirus infects the squamous epithelium of the esophagus, leading to ulceration (Fig. 2.25). The ulcer has a purulent base and well-demarcated edges. The characteristic cells with the viral cytopathic effect are usually located at the lateral borders of the ulcer. Infected cells and the cells surrounding the ulcer can be markedly reactive, occasionally mimicking dysplasia or malignancy.

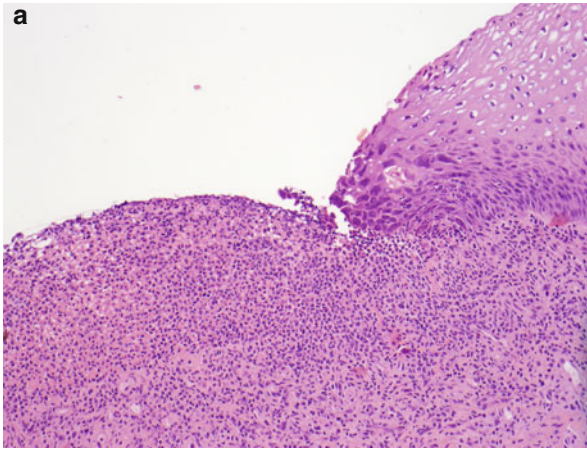
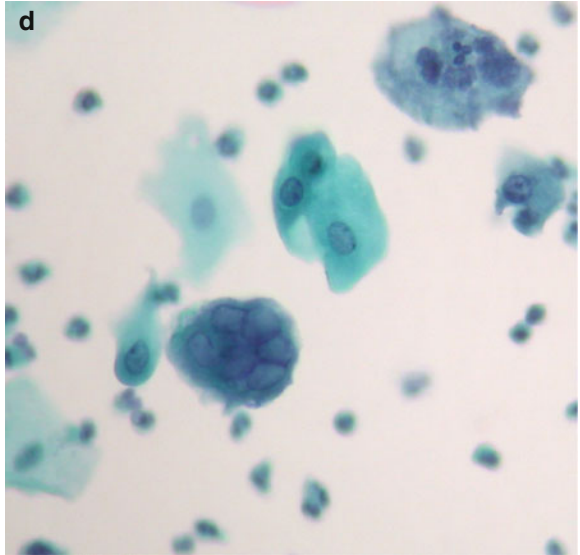
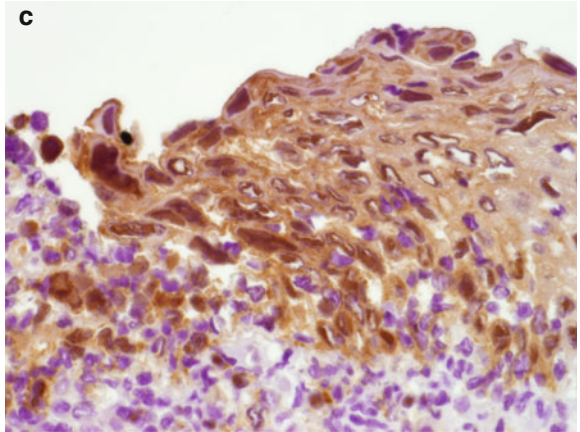
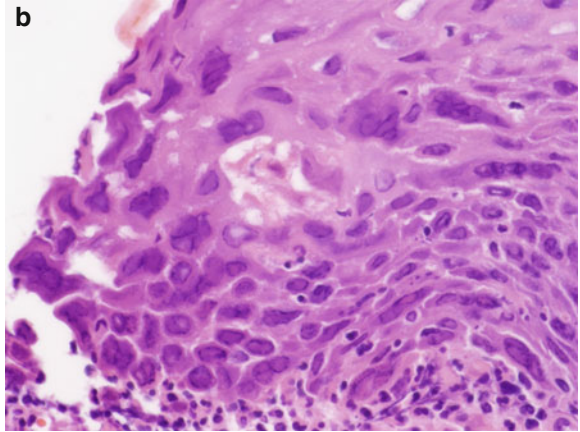


Fig. 2.25 (a) Herpes esophagitis (H & E, $\times 100$). (b) Herpes esophagitis (H & E, $\times 400$). Infected cells are enlarged, with nuclear molding, multinucleation, and margination of chromatin (the “three Ms” of herpesvirus infections). The nuclear membranes appear thickened because of the margination of chromatin. The nuclei have homogeneous, smooth chromatin, often referred to as having a “ground-glass” appearance. Some infected cells are mononuclear but still show ground-glass nuclei with chromatin margination. (c) Herpes esophagitis (immunohistochemical stain for HSV I and II, $\times 400$). The infected cells show dark brown nuclear staining. Immunohistochemistry helps highlight the characteristic cells in cases with relatively few cells or those lacking morphologically classic cells. (d) Herpesvirus cytopathic effect in esophageal brushing (ThinPrep, Papanicolaou stain, $\times 400$). The infected cells have a striking appearance in cytologic specimens, as seen in this esophageal brushing. The Papanicolaou stain demonstrates excellent nuclear detail. Note the prominent nuclear molding and fine homogeneous chromatin with margination

Fig. 2.25 (continued)



Squamous Papilloma

Exophytic squamous papilloma is characterized by papillary architecture, dilated vessels in the lamina propria, and elongation of the lamina propria papillae (Fig. 2.26) [11].

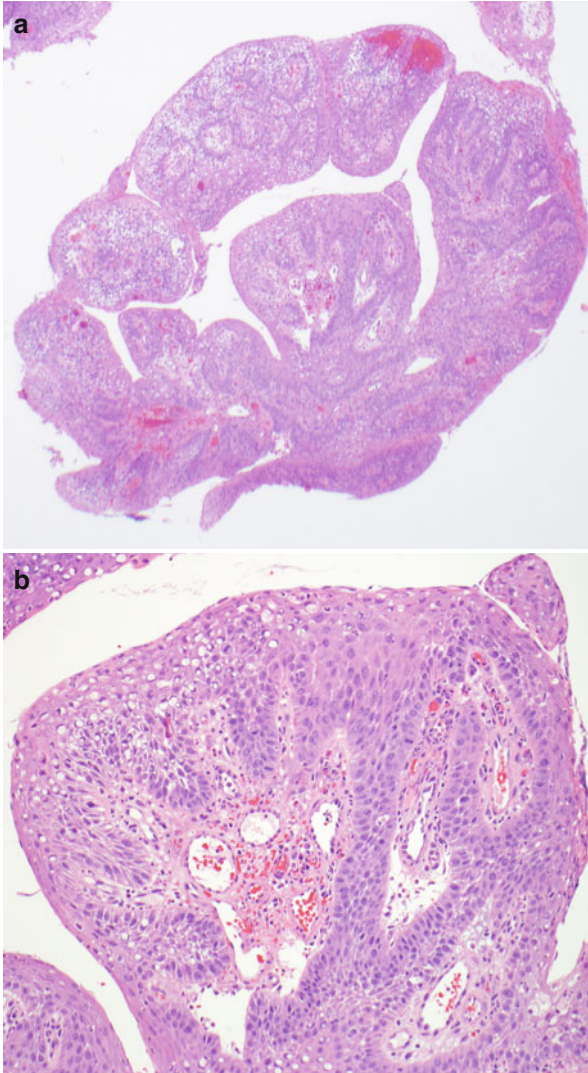


Fig. 2.26 Squamous papilloma. (a) H & E, ×20. (b) H & E, ×100. The squamous epithelial cells show reactive features including nuclear enlargement and hyperchromasia. Although many squamous papillomas are associated with HPV, diagnostic nuclear features are not seen in this example

References

1. Denardi FG, Riddell RH. Esophagus. In: Mills SE, editor. *Histology for pathologists*. 3rd ed. Philadelphia: Lippincott Williams and Wilkins; 2007. p. 565–88.
2. Noffsinger AE. Update on esophagitis: controversial and underdiagnosed causes. *Arch Pathol Lab Med*. 2009;133(7):1087–95.
3. Voltaggio L, Montgomery E, Lam-Himlin D. A clinical and histopathologic focus on Barrett esophagus and Barrett-related dysplasia. *Arch Pathol Lab Med*. 2011;135:1249–60.
4. Zhu W, Appelman HD, Greenson JK, Ramsburgh SR, Orringer MB, Chang AC, et al. A histologically defined subset of high-grade dysplasia in Barrett mucosa is predictive of associated carcinoma. *Am J Clin Pathol*. 2009;132:94–100.
5. Leers JM, DeMeester SR, Oezcelik A, Klipfel N, Ayazi S, Abate E, et al. The prevalence of lymph node metastasis in patients with T1 esophageal adenocarcinoma: a retrospective review of esophagectomy specimens. *Ann Surg*. 2011;235:271–8.
6. Edge SB, Byrd DR, Compton CC, Fritz AG, Greene FL, Trotti A, editors. *AJCC cancer staging handbook*. 7th ed. New York: Springer; 2010. p. 129–44.
7. Bosman FT, Carneiro F, Hruban RH, Theise ND, editors. *WHO classification of tumors of the digestive system*. Lyon: IARC; 2010.
8. Bennett AE, Goldblum JR, Odze RD. Inflammatory disorders of the esophagus. In: Odze RD, Goldblum JR, editors. *Surgical pathology of the GI tract, liver, biliary tract, and pancreas*. 2nd ed. Philadelphia: Saunders Elsevier; 2009. p. 231–67.
9. Genevay M, Rubbia-Brandt L, Rougemont A. Do eosinophil numbers differentiate eosinophilic esophagitis from gastroesophageal reflux disease? *Arch Pathol Lab Med*. 2010;134: 815–25.
10. Tang P, McKinley MJ, Sporrer M, Kahn E. Inlet patch: prevalence, histologic type, and association with esophagitis, Barrett esophagus, and antritis. *Arch Pathol Lab Med*. 2004;128: 444–7.
11. Lazenby A. Polyps of the esophagus. In: Odze RD, Goldblum JR, editors. *Surgical pathology of the GI tract, liver, biliary tract, and pancreas*. 2nd ed. Philadelphia: Saunders Elsevier; 2009. p. 406–7.